

Assessment of the two enantiomers of a metabolically stable radiotracer for imaging synaptic vesicle protein 2A in rat and monkey brains

Chao Zheng¹, Baosheng Chen¹, Takuya Toyonaga¹, Daniel Holden¹, Ming-Qiang Zheng¹, Jie Tong¹, Kyle C. Wilcox², Hong Gao¹, Krista Fowles¹, Jim Ropchan¹, Sjoerd J. Finnema², Richard E. Carson¹, Yiyun Huang¹, Zhengxin Cai¹

1. PET Center, Department of Radiology and Biomedical Imaging, Yale School of Medicine, New Haven, CT 06520, USA
2. Translational Imaging Neuroscience, AbbVie, North Chicago, IL 60064, USA

Abstract:

Objectives: Synaptic loss is one of the hallmarks of neurodegenerative diseases and region-specific changes in synaptic density are associated with a variety of neuropsychiatric diseases. To develop a metabolically stable analog of [^{11}C]UCB-A with improved membrane permeability and pharmacokinetics, we synthesized and evaluated [^{18}F]SDM-16 (**1**) for imaging of synaptic vesicle protein 2A (SV2A), a presynaptic marker ¹. In this study we prepared the enantiopure (*S*)-[^{18}F]SDM-16 (**2**) and compared its *in vivo* binding and imaging properties with [^{18}F]SDM-16 in rats and nonhuman primate (NHP).

Methods: A focused library of enantiopure SV2A ligands, selected labeling precursors and radiotracers were synthesized according to the reported procedures ^{1,2}. Binding affinities to human SV2A were measured through radioligand competition binding assays using [^3H]UCB-J. Baseline and levetiracetam blocking scans in rats and one rhesus monkey were performed on the Focus-220 scanner. In rats, whole brain time-activity curves (TACs) were generated for the baseline ($n = 3$) and blocking ($n = 3$) scans of both enantiomers. In NHP, arterial blood was drawn for metabolite analysis and construction of plasma input function. Regional brain TACs were fitted with one-tissue compartment (1TC) model to obtain K_1 , k_2 , and volume of distribution (V_T). Binding potential (BP_{ND}) was calculated using the nondisplaceable volume of distribution (V_{ND}) estimated from the blocking scan, where $BP_{\text{ND}} = (V_T/V_{\text{ND}}) - 1$. *In vivo* K_d ratio was calculated using the Guo plot ³ or BP_{ND} data, with $K_d(\mathbf{1})/K_d(\mathbf{2}) = BP_{\text{ND}}(\mathbf{2})/BP_{\text{ND}}(\mathbf{1})$.

Results: The ligand SDM-16, with the highest SV2A binding affinity (K_i 0.9 nM), and its enantiomer (*S*)-SDM-16 (K_i 25.2 nM) were chosen from a focused library of novel compounds for radiolabeling and evaluation. PET tracers **1** and **2** (**Fig. 1a**) were prepared from their respective enantiopure precursors in >99% radiochemical and enantiomeric purity, as determined by chiral radio-HPLC analysis. Molar activity at the end of synthesis was 283 ± 42 GBq/ μmol ($n=4$) for **1** and 170 ± 10 GBq/ μmol ($n=2$) for **2**. In rats the *S*-enantiomer showed much faster kinetics than the *R*-enantiomer, and the blocking studies confirmed SV2A specific binding of both tracers (**Fig. 1b**). In NHP, both tracers were metabolized slowly, with parent fraction of 68% (test) and 85% (retest) for **1** and 79% ($n=1$) for **2** at 120 min post-injection (**Fig. 1c**). Plasma free fraction (f_p) was 67% (test) and 65% (re-test) for **1**, and 64% for **2**. The plasma PK profiles of both tracers were very similar (**Fig. 1d**). Tracer **1** showed higher brain uptake and slower kinetics than **2** (**Fig. 1b, 1e**), consistent with the higher *in vitro* binding affinity of **1** than **2**. Both enantiomers have similar K_1 values (0.14), while tracer **2** has higher k_2 value (0.025) than **1** (0.007). TACs in NHP were well fitted with the 1TC model to derive regional V_T values, which ranged from 3.99 to 7.40 mL/cm³ for **2**, about 3.9-fold lower than those of **1**. BP_{ND} values were calculated to be from 2.58 to 12.26 for **1** and from 0.66 to 2.12 for **2** (**Table 1**). Based on the BP_{ND} data, the *in vivo* K_d ratio of **1** to **2** was 0.17 ± 0.02 , comparable to the ratio (0.2, **Fig. 1f**) derived from the Guo plot, but higher than the ratio of *in vitro* K_i measured with human SV2A (0.04).

Conclusions: In the brain of both rats and NHP, the two enantiomers displayed SV2A specific binding with differing kinetics, which was much faster for the *S*-enantiomer. In NHP both enantiomers showed similarly high metabolic stability, nearly identical metabolite-corrected input function, and plasma free fraction, while the *S*-enantiomer showed five-fold higher *in vivo* K_d value than the *R*-enantiomer. Quantitative analysis of the PET data demonstrated higher *in vivo* specific binding (BP_{ND}) of the *R*-enantiomer in NHP brain.

Figure:

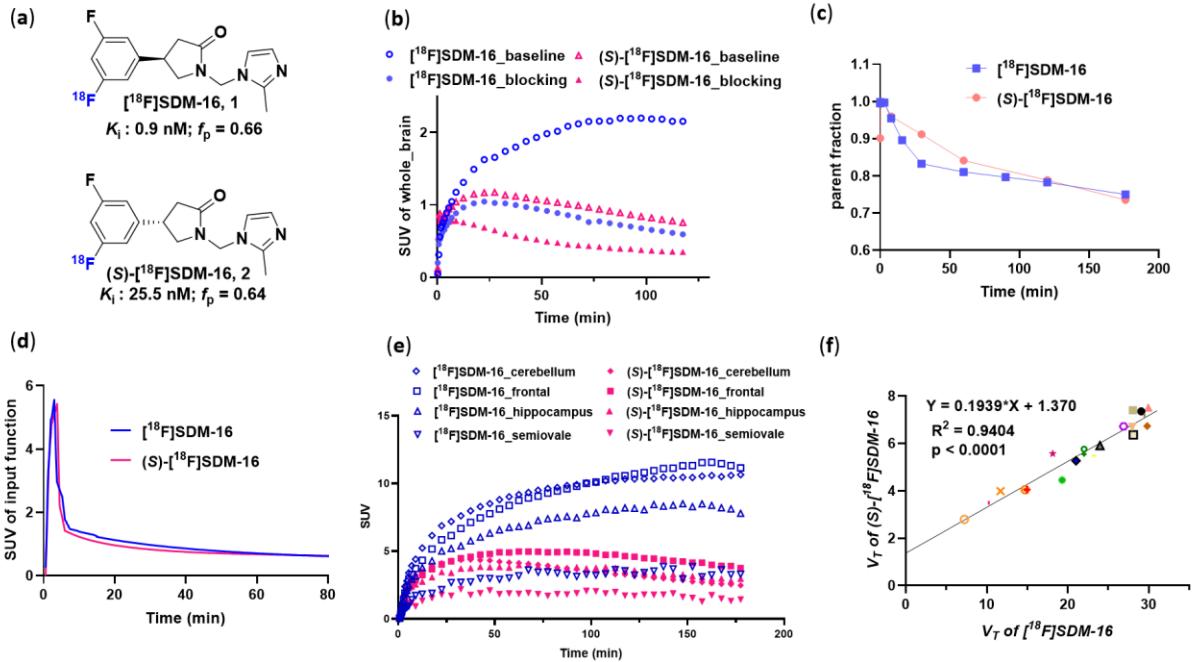


Figure 1. (a) Structure of the SV2A ligands $[^{18}\text{F}]\text{SDM-16}$ (**1**) and $(S)\text{-}[^{18}\text{F}]\text{SDM-16}$ (**2**); (b) Representative whole-brain TACs of **1** and **2** in Fischer 344 rats under baseline and blocking (levetiracetam, 3.33 mg/kg, i.v.) conditions; (c) Plasma parent fraction over time, (d) metabolite-corrected input function, and (e) representative brain regional time-activity curves of **1** and **2** in the same monkey; (f) Correlation and linear regression analysis of the baseline 1TC V_T values for **1** and **2** in the same monkey.

Table 1: Regional binding potentials (BP_{ND}) of [^{18}F]SDM-16 (n=2) and (S)-[^{18}F]SDM-16 (n=1) in the same rhesus monkey brain.

Radiotracer	[^{18}F]SDM-16 (test/retest)	(S)-[^{18}F]SDM-16
Cingulate cortex	11.65/9.22	2.05
Frontal cortex	11.30/8.76	2.07
Insular cortex	12.26/9.31	2.12
Nucleus accumbens	10.91/9.10	1.78
Occipital cortex	12.00/9.45	1.79
Temporal cortex	10.88/8.28	1.79
Putamen	11.39/8.72	1.64
Caudate	9.58/7.29	1.45
Thalamus	8.79/6.53	1.35
Cerebellum	8.18/6.36	1.19
Hippocampus	7.03/5.25	1.31
Globus pallidus	7.40/5.79	0.85
Brainstem	5.40/4.36	0.68
Amygdala	4.63/2.58	0.66

- 1 Zheng, C. *et al. EJNMMI* 2021; doi:10.1007/s00259-021-05597-5
- 2 Pracitto, R. *et al. ACS Omega* 2021; **6**:27676
- 3 Guo, Q. *et al. JCBFM* 2021; **34**:1162

For reviewer only:

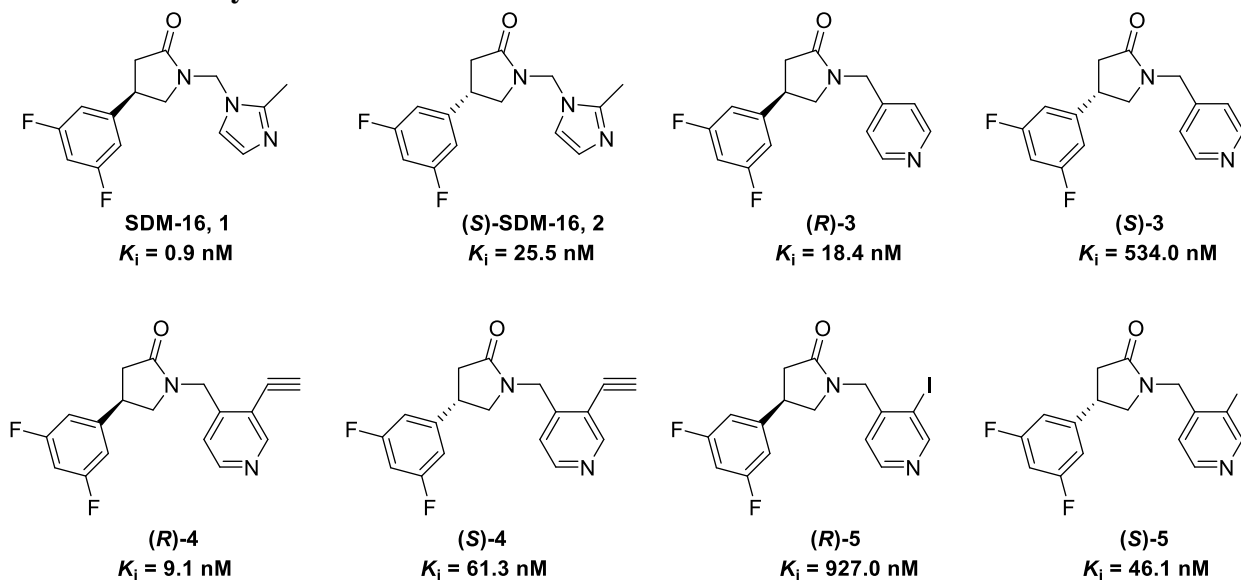


Fig. S1. Novel enantiopure SV2A ligands and their binding affinities to human SV2A